

Radiologic-Pathologic Correlation

Ocular Melanoma

Karen A. Tong, Anne G. Osborn,¹ Nick Mamalis, Roger P. Harrie, and N. Branson Call

From the Departments of Radiology and Ophthalmology, University of Utah School of Medicine, Salt Lake City, UT (AO, NM, RPH, NBC); and the Department of Radiology, Loma Linda University Medical Center, Loma Linda, CA (KT)

History

Clinical

A 65-year-old white man had impaired visual acuity in his left eye that persisted for 1 year. Examination revealed a small 2 × 3-mm cream-colored elevated left submacular nodule. Fluorescein angiography disclosed a choroidal lesion that suggested metastatic tumor. Laboratory tests were normal. At 6-month follow-up there was no evidence of progression. One year later, the patient complained of left proptosis (Fig 1) and worsening visual acuity. Ophthalmoscopy showed a large amelanotic mass filling the left posterior segment (Fig 2).

Imaging

A-mode ultrasound demonstrated a steep spike corresponding to the tumor surface (Fig 3A, *t*) anterior to the scleral spike (Fig 3A, *S*). During the ultrasound examination, spontaneous rapidly oscillating internal echoes were also observed, denoting vascularity within the mass. Low reflective echoes posterior to the scleral spike indicated an extraocular component (Fig 3A, *e*). On the B-mode study a collar-button-shaped solid intraocular mass (Fig 3B, *t*) with a hypoechoic base and a large relatively

sonolucent extrascleral retrobulbar component was seen (Fig 3B, *e*).

Precontrast computed tomographic (CT) scan disclosed a hyperdense left orbital mass (Fig 4A, *outlined arrows*) composed of a small intraocular component and a larger retro-orbital mass. Minimal enhancement after contrast administration was observed (Figs 4B–4D). The optic nerve (Fig 4D, *black arrowheads*) was surrounded by tumor. Intracranial CT was normal. Left orbital exenteration was performed.

Pathology

Gross pathology showed a mildly pigmented mushroom-shaped choroidal lesion that displaced the retina anteriorly almost to the posterior lens capsule (Figs 5A, 5B, and 6). The tumor extended around the optic nerve without invading the dural sheath. A slightly more pigmented large extrascleral component had extensive central hemorrhage and necrosis.

Microscopic examination revealed predominantly fusiform cells with spindle-shaped nuclei and prominent nucleoli. These spindle cells were interspersed with larger pleomorphic epithelioid cells (Fig 7).

Diagnosis

Predominantly amelanotic ocular melanoma (mixed spindle-B and epithelioid type).

Discussion

Incidence and Age

With an incidence of six per million per year, ocular melanomas are the most common pri-

Received April 13, 1993; accepted June 21.

¹ Address reprint requests to Anne G. Osborn, MD, Department of Radiology, University of Utah Medical Center, 50 North Medical Drive, Salt Lake City, UT 84132.

Index terms: Melanoma; Eyes, neoplasms; Eyes, ultrasound; Eyes, magnetic resonance; Radiologic-pathologic correlations

AJNR 14:1359–1366, Nov/Dec 1993 0195-6108/93/1406–1359

© American Society of Neuroradiology



Fig. 1. Clinical examination shows mild left proptosis. The abnormal fundus is indicated by the *white arrow*.

mary intraocular malignancy in adults (1). They are the second most common intraocular neoplasm overall, after metastasis. Ocular melanomas are generally unilateral, although bilateral melanomas occur sporadically (2). There is a slight male predominance and an eightfold higher incidence in whites than blacks. The median age at diagnosis is 55 years, with 70% of cases presenting in the fifth to seventh decade. Ocular melanoma is rare in childhood (1).

Etiology

Ocular melanoma is not considered an inherited disease, although recent studies suggest a genetic component. Possible predisposing factors include preexisting nevi, other melanocytic conditions such as ocular melanosis and nevus of Ota, impaired immunity, light-colored irides, occupational exposure (eg, welding), and trauma (1, 3).

Definition and Location

Melanomas are malignant neoplasms of melanocytes. Ocular melanomas occur in the most vascular part of the globe, the uvea. The uvea is the middle layer of the wall of the eye and is composed of the choroid, ciliary body, and iris. Ocular melanoma most commonly occurs in the choroid (85%); 9% and 6% arise in the ciliary body and iris, respectively (4). Melanoma rarely involves the conjunctiva, eyelid, or nasolacrimal duct (3).

Gross Pathology

Melanomas are divided into amelanotic or melanotic types by macroscopic visualization of pigmentation. Most melanomas have homogeneous texture, although larger tumors may be hemorrhagic or necrotic.

Choroidal melanomas are usually located posteriorly and are classified by size. Small tumors (less than 10 mm) are typically discoid and confined to the choroid. Medium-sized tumors (11 to 15 mm) usually have a classic collar-button or mushroom appearance. This is secondary to tumor herniation through a ruptured Bruch membrane, the transparent layer between the retinal pigment epithelium and the choroid (Fig 6). Larger tumors (greater than 15 mm) can fill the globe and extend through the sclera.

Ciliary melanomas tend to be small and may invade the anterior angle and iris. Iris melanomas are also small and can extend into the ciliary body or seed the anterior chamber (5).

Microscopic Pathology

There are two basic melanoma cell types: spindle and epithelioid. Spindle cells are fusiform in shape and are arranged in tight cohesive bundles with a syncytial appearance. Their cytoplasm has a fibrillar character. Spindle-A nuclei are thin with longitudinal folds or stripes, whereas spindle-B nuclei are larger and more oval with prominent nucleoli. Epithelioid cells

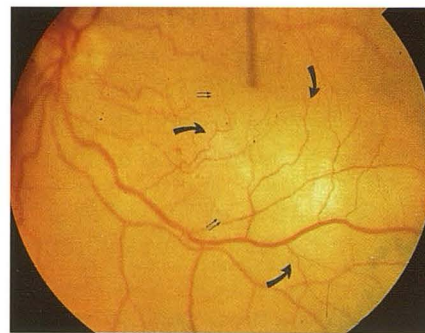


Fig. 2. Ophthalmoscopy shows a large amelanotic submacular choroidal mass (*curved arrows*). The mass extends to the fovea with minimal peripheral pigmentation (*double arrows*).

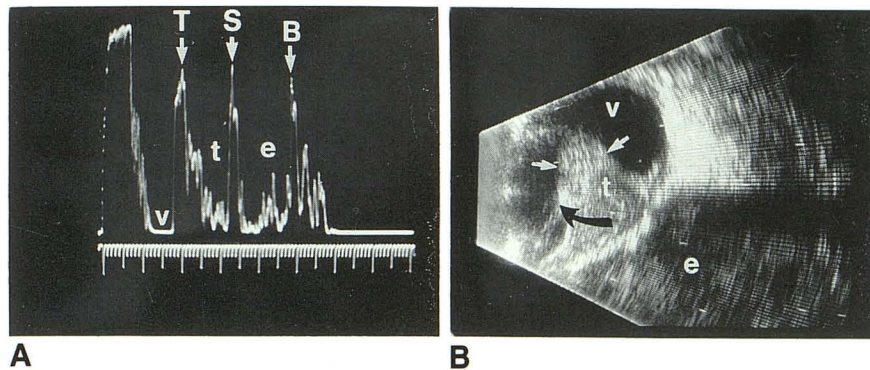


Fig. 3. A, A-mode ultrasound shows a steep spike of tumor surface with subsequent decreasing echoes anterior to the scleral spike. Posteriorly, low reflective echoes indicate extraocular tumor. *v* indicates vitreous body; *T*, tumor surface; *t*, tumor; *S*, sclera; *e*, extraocular tumor; and *B*, bone.

B, B-mode ultrasound shows solid collar-button-shaped intraocular mass (*arrows*) with large retrobulbar extension. The *curved black arrow* indicates penetration of tumor through the Bruch membrane. *v* indicates vitreous body; *t*, tumor; *S*, scleral; and *e*, extraocular component.

are large, pleomorphic, and occasionally multinucleated. These cells have distinct borders, abundant glassy cytoplasm, large round nuclei, irregular nuclear envelopes, coarse marginated nuclear chromatin, and larger eosinophilic central nucleoli. They tend to have greater mitotic activity. In addition to spindle (A and B) and epithelioid melanomas, there are mixed and necrotic types (5).

Associated Findings

Ocular melanoma is often associated with exudative retinal detachment (6) extending from the tumor margins and over the apex (7). Diffuse vitreous hyperintensity on magnetic resonance (MR) is occasionally seen (8, 9), which may be caused by increased protein from an impaired blood-retinal barrier, vitritis, or breaching of the Bruch membrane by the tumor.

Diagnosis

Clinical Presentation

Presenting signs and symptoms of ocular melanoma include decreased visual acuity, field defects, blurred vision, floaters, photopsia, and ocular pain. Many patients are asymptomatic, and diagnosis is made incidentally during routine examination (10). Ocular melanoma is suspected when a visible subretinal mass or exudative retinal detachment is seen by ophthalmoscopy. Fluorescein angiography shows hypervascularity.

Ocular Ultrasound

A-mode characteristics include a fixed solid mass, low to medium reflectivity, and regular vascularity (seen dynamically as spontaneous rapid spike movements). Small melanomas have uniform echo texture. Larger tumors attenuate sound, resulting in progressively decreasing echo amplitude through the tumor (Fig 3A, *t*). Extrascleral tumor is depicted by low reflective echoes in the orbit (Fig. 3A, *e*), posterior to the scleral spike (Fig. 3A, *S*) (7).

B-mode findings include characteristic mushroom or collar-button shape (Fig 3B) and choroidal excavation (loss of normally highly reflective choroid echoes) (11). Large tumors show echolucency in the tumor base because of sound attenuation and can be heterogeneous secondary to hemorrhage or necrosis (12). Coexisting retinal detachment is commonly seen extending from the tumor margins and over the tumor apex. Extrascleral extension is usually small and nodular adjacent to the tumor base but occasionally can be large. Rarely calcification occurs as a small focus on the surface, underlying localized retinal detachment (7).

CT

On CT, ocular melanoma appears as a focal, sharply marginated, elevated mass hyperdense to vitreous with mild to moderate enhancement after intravenous administration of contrast material (6, 9). The appearance on CT is non-specific.

Fig. 4. A, Precontrast axial CT shows hyperdense oblong, left orbital mass (arrows). The lesion has both an intraocular and retrobulbar component.

B-D, Postcontrast axial CTs show mild homogeneous enhancement of the lesion. Note anterior displacement of the sclera (double black arrows) by the large extraocular component. The optic nerve and sheath (black arrowheads) can be faintly seen surrounded by the tumor.

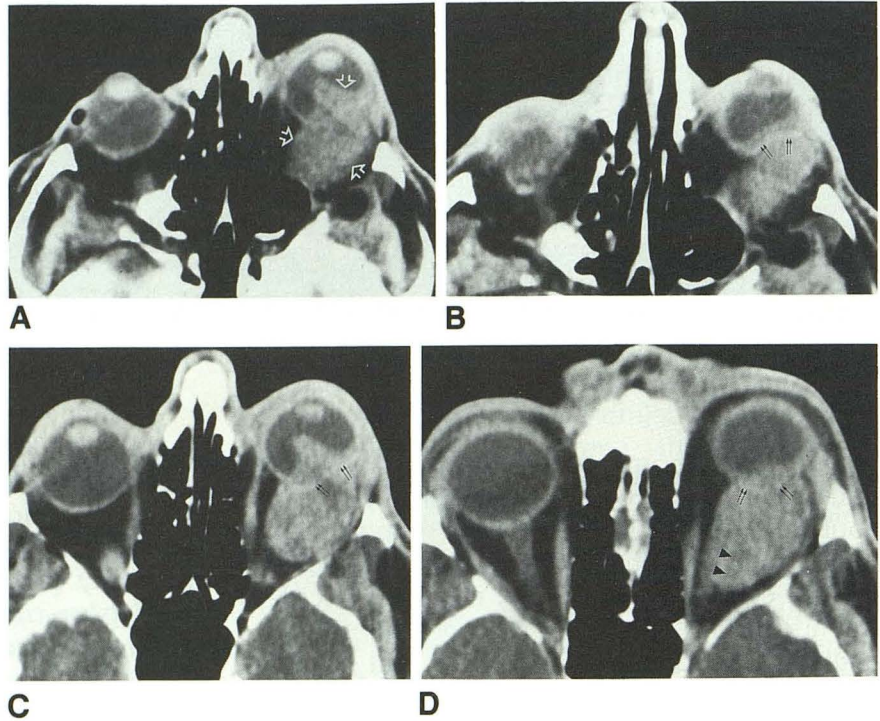
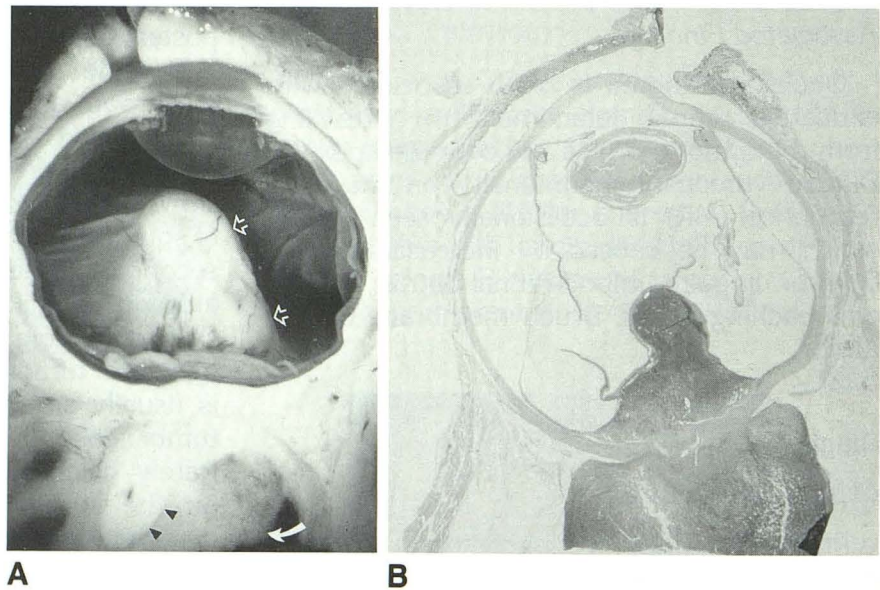


Fig. 5. A, Gross pathologic specimen shows a minimally pigmented mushroom-shaped choroidal mass (outlined arrows) that displaces the retina anteriorly, almost to the posterior lens capsule. A slightly more pigmented extrascleral component (curved white arrows) surrounds the optic nerve (black arrowheads).

B, Low-power magnification whole-mount specimen shows choroidal melanoma arising from the posterior globe, with large extrascleral extension. The characteristic collar-button or mushroom shape is caused by rupture and herniation through the Bruch membrane (see Fig 6).



MR

Early MR studies reported that melanomas demonstrated marked T1 shortening compared with other malignant tumors (11). Melanin has paramagnetic properties thought to be

secondary to stable free radicals that have dipole-dipole interactions with protons. Subsequent proton relaxation enhancement results in equal shortening of both T1 and T2 relaxation times. Therefore, ocular melanomas should display high signal on short-repetition-

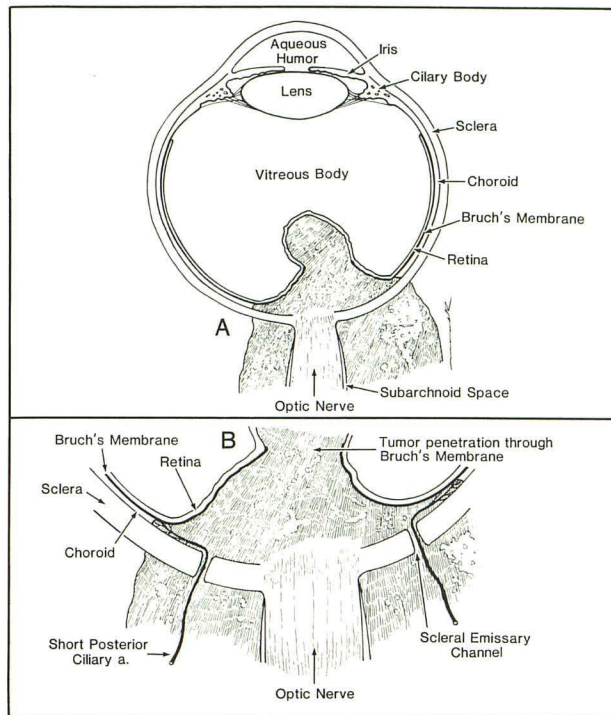


Fig. 6. Diagrammatic representation of Fig 5B.

B, Magnified view shows tumor penetration through the Bruch membrane and extrascleral extension through emissary channels for neurovascular structures such as the short-posterior choroidal arteries.

time/short-echo-time images and lower signal on long-repetition-time/short-echo-time images (4). This has been confirmed by most MR studies (9, 13–22).

More recent studies have reported a wider spectrum of MR signal patterns for melanoma (8, 23). One study demonstrated that T1 values of melanomas varied proportionally with field strength. Conversely higher melanin content has been associated with decreased T1 and T2 relaxation times (24). However, grossly amelanotic tumors also may produce T1 shortening, perhaps because of microscopic amounts of melanin (22). Other studies have reported variable appearance of amelanotic melanomas on MR (16, 18). Therefore, signal intensity may vary with field strength and may not be solely related to melanin content.

Melanoma can be complicated by hemorrhage or necrosis. Ocular melanoma and subacute hemorrhage both can have high sig-

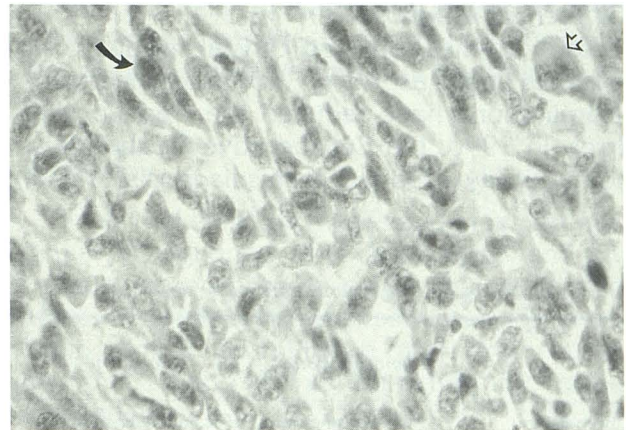


Fig. 7. High-power magnification demonstrates primarily fusiform-shaped cells (*curved arrow*) characteristic of spindle-B melanoma, although several large pleomorphic epithelioid cells (*outlined arrow*) are also seen, indicating mixed melanoma.

nal on T1-weighted images. On T2-weighted images, earlier hemorrhage is typically hypointense, whereas later hemorrhage is hyperintense, and melanin tends to be mildly hypointense (6).

MR can be helpful in differentiating between melanoma and subretinal fluid. Subretinal exudates typically appear hyperintense on both T1- and T2-weighted images because of high protein content (9, 16, 17, 21, 22). However, subretinal fluid itself also can be complicated by hemorrhage.

Several lesions can mimic the MR appearance of uveal melanoma. These include melanocytoma, retinoblastoma, choroidal hemorrhage, subretinal hemorrhage, subretinal fibrosis, senile disciform macular degeneration, and choroidal metastasis (8, 22). T1 shortening may be secondary to mucin, other proteinaceous fluid, or hemorrhage. Therefore, the T1 and T2 shortening in uveal melanoma should not be considered pathognomonic (8).

Several studies report difficulty demonstrating lesions less than 2 to 3 mm on MR (9, 14, 15, 17, 22). Small lesions or subtle extrascleral extensions not identified on MR have been detected by ultrasound (19). MR contrast agents increase the visibility of small tumors (8, 16, 25, 26).

Differential Diagnosis

Early studies reported clinical misdiagnosis rates as high as 40%. Accurate diagnostic examinations have reduced the frequency of error. In 1990, the Collaborative Ocular Melanoma Study reported a misdiagnosis rate of

0.48% (27). However, several ocular diseases continue to mimic uveal melanoma clinically, most commonly choroidal nevi, benign melanocytoma, choroidal hemangioma, choroidal hemorrhage, and choroidal metastasis (6, 28) (Table 1).

TABLE 1: Differential diagnosis of intraocular mass in adult

	Ophthalmoscopy	Ultrasound	CT	MR		Contrast Enhancement
				T1-Weighted	T2-Weighted	
Choroidal melanoma	Variably pigmented circumscribed mass of variable size; may have overlying retinal detachment	B-scan: collar-button or mushroom-shaped mass with regular texture A-scan: low to medium regular reflectivity often with spontaneous vascular pulsations Orbital echolucency in extrascleral extension	Focal mass hyperdense to vitreous	Moderate to marked hyperintensity to vitreous	Isointense or hypointense to vitreous	Mild to moderate
Choroidal nevus	Flat or minimally elevated gray lesions with slightly indistinct margins	B-scan: slightly elevated mass with regular texture A-scan: high internal reflectivity without spontaneous pulsations	Usually too small to be detected	Usually too small to be detected without contrast		Mild to moderate
Choroidal metastasis	Yellow to golden brown mildly elevated mass with irregular surface and borders; may have overlying retinal detachment; may be multiple, bilateral	B-scan: dome-shaped mass with irregular texture A-scan: irregular internal reflectivity usually without spontaneous pulsations	Focal thickening or mass	Variable	Variable	Mild to moderate
Choroidal hemangioma	Orange-red mildly elevated mass; may have overlying retinal detachment	B-scan: mildly elevated dome shaped mass with regular texture A-scan: high regular internal reflectivity without vascular pulsations Occasional calcification	Ill-defined mass	Variable	Variable	Intense
Subretinal or sub-choroidal hemorrhage	Round globular dark brown or green-brown mass	B-scan: dome-shaped, mildly elevated with variable texture A-scan: variable internal reflectivity; may have spontaneous pulsations; mobility of surface spike (may be subtle)	Focal mass hyperdense to vitreous	Variable	Variable	None

Prognosis and Treatment

Natural History and Prognosis

Extrascleral local extension occurs via scleral emissary channels for neurovascular structures and is associated with increased risk of recurrence (6) and hematogenous dissemination (5). Metastasis usually occurs hematogenously and is more common with choroidal melanomas (1). The liver is the most common remote site of metastasis (5). Other sites include the lung, spine, skin, subcutaneous tissue, nodes, brain and adrenal (29, 30). Metastasis usually occurs within five years of presentation and occasionally after long intervals. Rarely optic nerve invasion can result in intracranial metastasis (31, 32).

Uveal melanoma is a potentially fatal disease in adults. The 5-, 10-, and 15-year survival rates are 65%, 52%, and 46%, respectively. The median survival after hepatic metastasis is 2 to 4 months (1). Epithelioid cell type and tumor diameter greater than 10 mm indicate poor prognosis. Other indicators of poor prognosis include elevated mitotic rate, diffusely infiltrating tumor, scleral/extrascleral extension, necrosis, and lymphocytic infiltration (5, 8).

Therapy

Treatment is largely determined by tumor size. Other important factors include tumor location, tumor activity, status of the contralateral eye, age, general health, and presence of metastasis. Although the traditional method of treatment has been enucleation, currently most small dormant tumors without extrascleral extensions are managed conservatively and followed by ultrasound observation. Local en-bloc resection has been performed for small anterior uveal lesions. Laser photocoagulation is occasionally used for small choroidal melanomas. Radiation therapy (radioactive plaque therapy or external beam irradiation) is performed for many medium-sized and even some large melanomas. Exenteration for extensive or recurrent tumor is performed sometimes, although prognosis is poor. Metastatic mela-

noma has been treated with chemotherapy with minimal effect. Experimental therapies include hyperthermia and immunotherapy (5, 33).

Summary

Uveal melanoma is the second most frequent ocular malignancy after metastasis and the most common primary ocular malignant neoplasm in adults. The diagnosis is usually made from clinical examination and ocular ultrasound. CT and MR may be helpful for further evaluation.

References

1. Egan KM, Seddon JM, Glynn RJ, et al. Major review: epidemiologic aspects of uveal melanoma. *Surv Ophthalmol* 1988;32:239-251
2. Seregard S, Daunius C, Kock E, Popovic V. Two cases of primary bilateral malignant melanoma of the choroid. *Br J Ophthalmol* 1988;72:244-245
3. Rennie IG. Diagnosis and treatment of ocular melanomas. *Br J Hosp Med* 1991;46:144-156
4. Char DH, Umsold R, Sobel DF, et al. Computed tomography: ocular and orbital pathology. In: Newton TH, Bilaniuk LT, eds. *Modern neuroradiology. Vol. 4: Radiology of the eye and orbit*. Kentfield, Calif: Raven, 1990:9.4-9.5
5. McLean IW, Bernier MN, Zimmerman LE, Jakobiec FA. *Tumors of the eye and ocular adnexae: atlas of tumor pathology*. 3rd series. Washington, DC: Armed Forces Institute of Pathology (in press)
6. Atlas S. *Magnetic resonance imaging of the brain and spine*. New York: Raven, 1991:721-724
7. Byrne SF, Green RL. *Ultrasound of the eye and orbit*. St. Louis: Mosby-Year Book, 1992:134-173
8. Bloom PA, Ferris JD, Laidlaw DAH, Goddard PR. Magnetic resonance imaging: diverse appearances of uveal malignant melanomas. *Arch Ophthalmol* 1992;110:1105-1111
9. Mafee MF, Peyman GA, Grisolano JE, et al. Malignant uveal melanoma and simulating lesions: MR imaging evaluation. *Radiology* 1986;160:773-780
10. Servodidio CA, Abramson DH. Presenting signs and symptoms of choroidal melanoma: what do they mean? *Ann Ophthalmol* 1992;24:190-194
11. Hodes BL. Ultrasonographic diagnosis of choroidal malignant melanoma. *Surv Ophthalmol* 1977;22:29-40
12. Munk PL, Vellet AD, Levin M, et al. Sonography of the eye. *AJR: Am J Roentgenol* 1991;157:1079-1086
13. Damadian R, Zaner K, Hor D, DiMaio T. Human tumors detected by nuclear magnetic resonance. *Proc Natl Acad Sci USA* 1974;71:1471-1473
14. Chambers RB, Davidorf FH, McAdoo JF, Chakeres DW. Magnetic resonance imaging of uveal melanomas. *Arch Ophthalmol* 1987;105:917-921
15. Mafee MF, Peyman GA, Peace JH, et al. Magnetic resonance

- imaging in the evaluation and differentiation of uveal melanoma. *Ophthalmology* 1987;94:341-348
16. Mihara F, Gupta KL, Murayama S, et al. MR imaging of malignant uveal melanoma: role of pulse sequence and contrast agent. *AJNR: Am J Neuroradiol* 1991;12:991-996
 17. Peyman GA, Mafee MF. Uveal melanoma and similar lesions: the role of magnetic resonance imaging and computed tomography. *Radiol Clin North Am* 1987;24:471-486
 18. Peyster RG, Augsburger JJ, Shields JA, et al. Intraocular tumors: evaluation with MR imaging. *Radiology* 1988;168:773-779
 19. Raymond WR, Char DH, Norm D, Protzko EE. Magnetic resonance imaging evaluation of uveal tumors. *Am J Ophthalmol* 1991;111:633-641
 20. Sobel DF, Kelly W, Kjos BO, et al. MR imaging of orbital and ocular disease. *AJNR: Am J Neuroradiol* 1985;6:259-264
 21. Sullivan JA, Harms SE. Surface-coil MR imaging of orbital neoplasms. *AJNR: Am J Neuroradiol* 1986;7:29-34
 22. Wilms G, Marchal G, Van Fraeyenhoven L, et al. Shortcomings and pitfalls of ocular MRI. *Neuroradiology* 1991;33:320-325
 23. Marx HF, Colletti PM, Raval JK, et al. Magnetic resonance imaging features in melanoma. *Magn Reson Imaging* 1990;3:223-239
 24. Gomori JM, Grossman RI, Shields JA, et al. Choroidal melanomas: correlation of NMR spectroscopy and MR imaging. *Radiology* 1986;158:443-445
 25. Adam G, Brab M, Bohndorf K, Gunther RW. Gadolinium-DTPA-enhanced MRI of intraocular tumors. *Magn Reson Imaging* 1990;8:683-689
 26. Bond JB, Haik BG, Mihara F, Gupta KL. Magnetic resonance imaging of choroidal melanoma with and without gadolinium contrast enhancement. *Ophthalmology* 1991;98:459-466
 27. Albert DM. Accuracy of diagnosis of choroidal melanomas in the collaborative ocular melanoma study. *Arch Ophthalmol* 1990;108:1268-1273
 28. Shields JA, Augsburger JJ, Brown GC, Stephens RF. The differential diagnosis of posterior uveal melanoma. *Ophthalmology* 1980;87:518-522
 29. Lorigan JG, Wallace S, Mavligit GM. The prevalence and location of metastases from ocular melanoma: Imaging study in 110 patients. *AJR: Am J Roentgenol* 1991;157:1279-1281
 30. Shields JA, Shields CL, Shakin EP, Kobetz LE. Metastasis of choroidal melanoma to the contralateral choroid, orbit, and eyelid. *Br J Ophthalmol* 1988;72:456-460
 31. Al-Haddab S, Hidayat A, Tabbara KF. Ciliary body melanoma with optic nerve invasion. *Br J Ophthalmol* 1990;74:123-124
 32. Jones DR, Scobie IN, Sarkies NJC. Intracerebral metastases from ocular melanoma. *Br J Ophthalmol* 1988;72:246-247
 33. Shields JA, Shields CL, Donoso LA. Major review: management of posterior uveal melanoma. *Surv Ophthalmol* 1991;36:161-195